Black holes and nilmanifolds: quasinormal mode calculations

Anna Chrysostomou[1,2], Alan S. Cornell[1], Aldo Deandrea[2], Étienne Ligout[3], and Dimitrios Tsimpis[2]

[1] Department of Physics, University of Johannesburg, PO Box 524, Auckland Park 2006, South Africa
[2] Institut de Physique des Deux Infinis de Lyon, Université de Lyon, UCBL, UMR 5822 CNRS/IN2P3, 4 rue Enrico Fermi, 69622 Villeurbanne Cedex, France
[3] École Normale Supérieure de Lyon, Site Monod, 46 Allée d'Italie, 69364 Lyon Cedex 07, France

E-mail: achrysostomou@uj.ac.za, acornell@uj.ac.za, deandrea@ipnl.in2p3.fr, etienne.ligout-de-oliveira1@ens-lyon.fr, tsimpis@ipnl.in2p3.fr

Abstract. In the wake of a perturbation, a n-dimensional black hole emits complex and characteristic oscillations in spacetime known as "quasinormal modes" (QNMs). These black hole QNMs have been used to explore beyond the Standard Model (BSM) scenarios and quantum gravity conjectures. With the establishment of the LIGO-Virgo-KAGRA network of gravitational-wave (GW) detectors, we find ourselves presented with the unprecedented opportunity to compare computed QNMs against GW data from binary black hole merger events. Encouraged by this development, we investigate whether QNMs can be exploited in the search for signatures of extra dimensions. To address a gap in the BSM literature, we focus here on higher dimensions with negative Ricci curvature. As a first step, we consider a direct space formed from a 4D Schwarzschild black hole spacetime and a 3D nilmanifold (twisted torus); we model the black hole perturbations as a scalar test field. We find that the extra-dimensional geometry can be included in the QNM effective potential as a squared mass-like term μ. We then calculate the corresponding QNM spectrum using three different numerical methods and determine a possible upper bound for a detectable μ.

1. Introduction

Within the context of general relativity, Birkhoff's theorem stipulates that the most general spherically-symmetric vacuum solution of the Einstein field equations is the Schwarzschild metric

$$\mathrm{d}s^2_{BH} = g^{\mathrm{BH}}_{\mu\nu}\mathrm{d}x^\mu \mathrm{d}x^\nu = -f(r)\,\mathrm{d}t^2 + f(r)^{-1}\,\mathrm{d}r^2 + r^2(\mathrm{d}\theta^2 + \sin^2\mathrm{d}\phi^2)\,, \tag{1}$$

where $f(r) = 1 - r_H/r$ and $r_H = 2M$ is the Schwarzschild event horizon. This metric describes an isolated, static, and neutral 4D black hole [1, 2] that is fully characterised by its mass M [3].

Astrophysically, black holes are perpetually in a perturbed state: even if somehow isolated from the fields and matter in their immediate vicinity, they interact with the surrounding vacuum through Hawking radiation. We may describe the perturbed black hole using the metric

$$g'_{\mu\nu} = g^{\mathrm{BH}}_{\mu\nu} + \delta_{\mu\nu}\,, \tag{2}$$

where the unperturbed black hole metric $g_{\mu\nu}^{\rm BH}$ is referred to as the "background" and the "perturbations" $\delta_{\mu\nu}$ are considered to be very small ($\delta_{\mu\nu} \ll g_{\mu\nu}^{\rm BH}$) at the lowest linear approximation [4]. In the wake of the perturbation, the black hole will emit gravitational radiation dominated by a discrete set of complex "quasinormal" frequencies (QNFs). The real part of these QNFs represent the physical oscillation frequency and the imaginary part is the inverse damping time. To model the perturbing field − known as the quasinormal mode (QNM) − we may consider a scalar test field evolving on a fixed background that contributes negligibly to the energy-density of the system.

Although dissipative systems are ubiquitous in nature, the black hole QNM boundary-value problem is of particular interest due to the physical origin of its damping and the characteristic black hole information that the QNFs convey.

The first of these features can be addressed by considering the black hole spacetime itself through the classical lens, where the presence of an event horizon $r_{_H}$ results in the irreversible loss of gravitational radiation to the black hole interior. Since gravitational radiation also cannot enter the system from beyond spatial infinity, we can then describe the QNM boundary conditions as purely ingoing at the horizon and purely outgoing at spatial infinity. The system is therefore not time-symmetric; the eigenvalue problem is non-Hermitian. In general, the corresponding eigenfunctions are then not normalisable and do not form a complete set (see reviews [4–6] for details).

The second feature, namely the relationship between QNMs and black hole characteristics, rests on the fact that black hole parameters like mass and spin can be accurately predicted from the QNF spectrum [7]. This has been a topic of interest within gravitational-wave (GW) research [8] and has been demonstrated successfully by the LIGO-Virgo-KAGRA collaboration [9–13].

Other more esoteric GW pursuits include searches for evidence of extra dimensions (see Ref. [14]), wherein which QNMs have recently been considered for a 5D braneworld case [15]. Here, we focus on an extra-dimensional setup in which a 4D Schwarzschild black hole is embedded into a 7D $\mathcal{M}_4 \times \mathcal{N}_3$ manifold, where $\mathcal{M}_4$ is the usual (3+1) flat spacetime and $\mathcal{N}_3$ is a negatively-curved compact space. Specifically, $\mathcal{N}_3$ here is a "nilmanifold" (twisted torus) fully characterised by the Heisenberg algebra, from which its geometric properties naturally follow (see section 2 for the nilmanifold's construction, detailed further in Ref. [16]).

In this work, we determine an upper bound under which black hole QNMs may serve as an appropriate probe for extra dimensions. This is made possible by expressing the extra-dimensional components of our 7D Schwarzschild-nilmanifold setup as an effective mass-like term in the QNM potential, and then exploiting QNM techniques to solve the corresponding wave equation.

2. The potential of a Schwarzschild-nilmanifold setup

While the parameter space of flat and positively-curved extra dimensions has been probed and constrained [17], models involving higher-dimensional manifolds with negative Ricci curvature have remained under-explored. Phenomenologically, studies on compact negative spaces suggest that these models could be used to address the hierarchy problem [18] and cosmological observations [19, 20]. These motivate our interest in the manifold $\mathcal{M}_4 \times \mathcal{N}_3$.

To construct $\mathcal{N}_3$, recall that any Lie group G of dimension d can be understood as a d-dimensional differentiable manifold. To make G compact, we quotient by the lattice Γ. A group for which such a Γ always exists is called a "nilpotent group". For $d = 3$, there is the trivial abelian algebra that leads to a three-torus, as well as three different solvable algebras. Of these, one is nilpotent: the Heisenberg algebra,

$$[Z_1, Z_2] = -\mathtt{f} Z_3 \ , \quad [Z_1, Z_3] = [Z_2, Z_3] = 0 \ , \tag{3}$$

where the structure constant $\mathtt{f} = -f^3{}_{12}$ is the "geometric flux" serving as the nilmanifold's "twist parameter". The corresponding geometric properties can be relayed through the Maurer-Cartan equation,

$$\mathrm{d}e^3 = \mathtt{f} e^1 \wedge e^2 \ , \ \ \mathrm{d}e^1 = 0 \ , \ \ \mathrm{d}e^2 = 0 \ , \tag{4}$$

$$\Rightarrow \ \ e^1 = r^1 \mathrm{d}y^1 \ , \ \ e^2 = r^2 \mathrm{d}y^2 \ , \ \ e^3 = r^3(\mathrm{d}y^3 + N r^1 \mathrm{d}y^2) \ , \tag{5}$$

where $N = r^1 r^2 \mathtt{f}/r^3$. In this way, the manifold is fully characterised and we can obtain the most general minimal left-invariant metric,

$$\mathrm{d}s^2_{nil} = \delta_{ab} e^a e^b = (r^1 \mathrm{d}y^1)^2 + (r^2 \mathrm{d}y^2)^2 + (r^3 \mathrm{d}y^3 + N r^1 r^3 \mathrm{d}y^2)^2 \tag{6}$$

From eqs. (1) and (6), we can construct our extra-dimensional manifold $ds^2_{7D} = ds^2_{BH} + ds^2_{nil}$. Exploiting the spherically-symmetrical context, the 7D propagating scalar field can be expressed as

$$\Psi^s_{n\ell m}(\mathbf{z}) = \sum_{n=0}^{\infty} \sum_{\ell,m}^{\infty} \ \frac{\psi_{sn\ell}(r)}{r} \ Y^s_{m\ell}(\theta, \phi) \ Z(y^1, y^2, y^3) \ e^{-i\omega t} \ , \tag{7}$$

where spherical harmonics in (θ, ϕ) are denoted by (ℓ, m), s represents the spin of the field, and n is the overtone number labelling the QNFs by increasing values of $|\mathbb{I}m\{\omega\}|$. To determine the QNM behaviour, we first apply the Laplacian. For this unusual spacetime, we can account for the higher dimensions by exploiting the separability of the metric. Recall that the Laplacian of a product space is the sum of its parts, such that

$$\nabla^2 \Psi(\mathbf{z}) = \left(\nabla^2_{BH} + \nabla^2_{nil}\right) \Phi^s_{n\ell m}(\mathbf{x}) Z(\mathbf{y}) \ . \tag{8}$$

However, if we choose to encode the higher-dimensional behaviour through an effective mass term representing a Kaluza-Klein tower of states, then we may describe the 7D scalar field evolution through a 4D "massive" Klein-Gordon equation,

$$\nabla^2_{\mathrm{nil}} Z(\mathbf{y}) = -\mu^2 Z(y^1, y^2, y^3) \quad \Rightarrow \quad \frac{1}{\sqrt{-g}} \partial_\mu \left(\sqrt{-g} g^{\mu\nu} \partial_\nu \Psi\right) - \mu^2 \Psi = 0 \ . \tag{9}$$

Using the tortoise coordinate $dr_* = dr/f(r)$, we extract the radial component of the QNM to produce a characteristic wavelike equation containing the QNF and the effective scalar potential,

$$\frac{d^2\psi}{dr_*^2} + \left(\omega^2 - V(r)\right) \psi = 0 \ , \qquad V(r) = \left(1 - \frac{2M}{r}\right) \left(\frac{\ell(\ell+1)}{r^2} + \frac{2M}{r^3} + \mu^2\right) \ . \tag{10}$$

Within the QNM literature, a modified WKB approach informed by the QNM boundary conditions [21, 22] serves as a well-established numerical method for solving eq. (10). At lowest order [21], this WKB method yields

$$\omega^2(\ell, n) \approx V(r_0) - i(n + 1/2)\sqrt{-2V''(r_0)} \ , \tag{11}$$

where derivatives with respect to r are denoted by primes and r_0 represents the peak of the potential. For low values of n, eq. (11) demonstrates that the QNF can be closely determined by the height of its associated potential barrier, as well as its second derivative [23, 24]. As such, we may visualise the influence of the mass-like term on the QNF by studying the potential (see figure 1). We observe that μ elevates the potential; as r_* increases, the potential no longer asymptotes to zero but instead approaches μ^2. Beyond $\mu \approx 0.6$, the peak is smoothed out, suppressing the potential barrier.

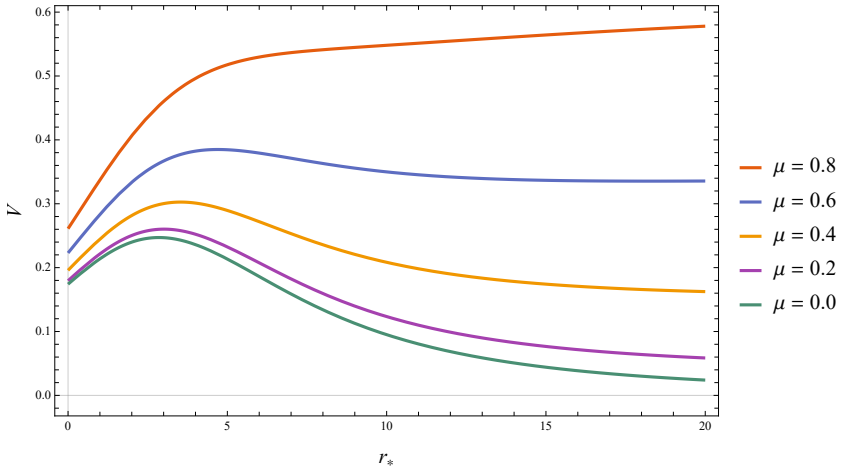

Figure 1: The scalar potential of eq. (10) for increasing values of the mass-like parameter μ. Note that for $\mu = 0$, $V \to \infty$ as $r_* \to \infty$ and the effective potential has a distinct peak. For $\mu \neq 0$, $V \to \mu^2$ as $r_* \to +\infty$; the curve is smoothed as μ grows and the potential barrier is lost.

3. Computing the QNF spectrum for the Schwazrschild-nilmanifold setup

From eq. (11), we observe that the QNF value is strongly influenced by the potential; from figure 1, we observe that for some critical μ, the QNM potential no longer retains its characteristic bell-like shape. To determine this μ, we compute the QNF spectrum using a higher-order WKB approach [22] and an analytical method wherein which we calculate QNFs from the inverted Pöschl-Teller potential [25]. We also employ a technique put forth by Dolan and Ottewill that solves eq. (10) with a novel, physically-motivated ansatz to produce QNFs as a series expansion in inverse powers of $L = \ell + 1/2$ [26]. The first two are well-known methods that rely on a barrier-shaped QNM potential to be effective [27]. We have studied the third extensively in the eikonal limit in Ref. [28]; here, we find that the QNF emerges as a function of both L and μ:

$$\begin{aligned}\omega(L,\mu) =& \frac{1}{3}L - \frac{i}{6}L^0 + \left[\frac{3\mu^2}{2} + \frac{7}{648}\right]L^{-1} + \left[\frac{5i\mu^2}{4} - \frac{137i}{23328}\right]L^{-2} \\ &+ \left[\frac{9\mu^4}{8} - \frac{379\mu^2}{432} + \frac{2615}{3779136}\right]L^{-3} + \left[\frac{27i\mu^4}{16} - \frac{2677i\mu^2}{5184} + \frac{590983i}{1088391168}\right]L^{-4} \\ &+ \left[\frac{63\mu^6}{16} - \frac{427\mu^4}{576} + \frac{362587\mu^2}{1259712} - \frac{42573661}{117546246144}\right]L^{-5} \\ &+ \left[\frac{333i\mu^6}{32} + \frac{6563i\mu^4}{6912} + \frac{100404965i\mu^2}{725594112} + \frac{11084613257i}{25389989167104}\right]L^{-6}\,.\end{aligned} \tag{12}$$

Our results are summarised in table 1, for which we set $\ell = 2$ and $n = 0$ to correspond to the least-damped/longest-lived "fundamental mode" that dominates the QNM signal [4, 6, 9]. We find that the sixth-order WKB and the Dolan-Ottewill methods are in close agreement. We can ascribe the deviations in the Pöschl-Teller results to the method's stronger reliance on the potential shape, where the Pöschl-Teller potential is known to match closest to the inverted potential corresponding to a Schwarzschild black hole spacetime with a positive cosmological constant [29].

From table 1, we observe that $\mathbb{R}e\{\omega\}$ increases steadily with μ whereas $\mathbb{I}m\{\omega\}$ decreases. As μ approaches 0.7, there is a discernible change in the QNF behaviour: a large jump in both the real and imaginary parts is observed for all three methods, with a pronounced difference

Table 1: We calculate the QNFs at $n = 0$ and $\ell = 2$ for $0.0 \leq \mu \leq 0.7$ using the WKB technique at $\mathcal{O}(V^6)$, the Pöschl-Teller (PT) method, and the Dolan-Ottewill (DO) expansion at $\mathcal{O}(L^{-6})$.

μ	$\omega\ (WKB)$	$\omega\ (PT)$	$\omega\ (DO)$
0.0	$0.4836 - 0.0968i$	$0.4874 - 0.0979i$	$0.4836 - 0.0968i$
0.1	$0.4868 - 0.0957i$	$0.4909 - 0.0968i$	$0.4868 - 0.0957i$
0.2	$0.4963 - 0.0924i$	$0.5015 - 0.0936i$	$0.4963 - 0.0924i$
0.3	$0.5123 - 0.0868i$	$0.5192 - 0.0881i$	$0.5124 - 0.0868i$
0.4	$0.5351 - 0.0787i$	$0.5443 - 0.0800i$	$0.5352 - 0.0787i$
0.5	$0.5649 - 0.0676i$	$0.5770 - 0.0690i$	$0.5653 - 0.0676i$
0.6	$0.6022 - 0.0528i$	$0.6181 - 0.0541i$	$0.6032 - 0.0532i$
0.7	$0.1396 + 0.2763i$	$0.6695 - 0.0312i$	$0.6500 - 0.0343i$

in the WKB result for $\mu = 0.7$: a sudden drop in $\mathbb{R}e\{\omega\}$ and shift from negative to positive in $\mathbb{I}m\{\omega\}$. Mathematically, we can attribute this behaviour as evidence of a breakdown in the methodology: since the local maximum is eradicated after $\mu = 0.6$ in fig. 1, it is impossible to carry out the WKB matching procedure beyond this μ value. This justification is supported by the QNM literature for fields of large mass (see the WKB review by Konoplya [27]).

However, there is also the physical interpretation to consider. Massive QNMs for which $\mathbb{R}e\{\omega^2\} > \mu^2$ are "propagative" and behave similarly to their massless counterparts, whereas QNMs for which $\mathbb{R}e\{\omega^2\} < \mu^2$ are "evanescent" and contribute negligibly to the QNM spectrum for a perturbed black hole. This shift from propagative to evanescent is characterised by a change in sign in the imaginary part [24]. As μ increases, the QNMs transition from propagative to evanescent; as the imaginary part goes to zero, the QNMs enter the "quasiresonance regime" [23, 30], where the QNMs are arbitrarily long-lived. In this regime, the ingoing wave amplitude at the event horizon of the black hole is considered much smaller than the amplitude far from the black hole; energy no longer "leaks" from the system at spatial infinity and the QNMs behave as standing waves [4].

In our extra-dimensional setup, the μ parameter serves as a manifestation of the extra dimensions. The analysis of the QNM potential and corresponding QNF spectrum conducted here demonstrates that only the "propagative" QNMs can be used as a probe in extra-dimensional searches. This places an upper bound on μ, such that $\mathbb{R}e\{\omega^2\} > \mu^2$. For a scalar test field in the Schwarzschild black hole spacetime, we require that $\mu < 0.6$.

4. Conclusions

In this work, we have considered a novel extra-dimensional setup comprised of a Schwarzschild black hole embedded in a 7D product spacetime whose extra dimensions form a negative compact space − specifically, a nilmanifold built from Heisenberg algebra. We have pursued a strategy for an extra-dimensional search using QNMs. By positioning the extra-dimensional contribution as an effective mass-like μ term in the QNM potential, we have demonstrated through a numerical study a possible upper bound on this μ.

In an ongoing investigation based on the parametric deviation of GWs from the QNMs predicted by general relativity, we suggest that this bound may be further constrained. Our next immediate step is to subject the mass spectrum of the nilmanifold model studied in Ref. [16] to this constraint in order to extract tangible bounds on the radius of the nilmanifold extra dimensions herein constructed.

Acknowledgments
ASC is supported in part by the National Research Foundation (NRF) of South Africa; AC is supported by the NRF and Department of Science and Innovation through the SA-CERN programme and a Campus France scholarship. EL is supported by the French Governement through the École Normale Supérieure de Lyon.

References

[1] Misner C W, Thorne K S and Wheeler J A 1973 *Gravitation* (San Francisco: W. H. Freeman)
[2] Chandrasekhar S 1983 *The Mathematical Theory of Black Holes* (New York: Oxford Univerity Press)
[3] Israel W 1967 *Phys. Rev.* **164**(5) 1776–9
[4] Konoplya R A and Zhidenko A 2011 *Rev. Mod. Phys.* **83** 793–836
[5] Nollert H P 1999 *Class. Quant. Grav.* **16** R159–R216
[6] Berti E, Cardoso V and Starinets A O 2009 *Class. Quant. Grav.* **26** 163001
[7] Echeverria F 1989 *Phys. Rev. D* **40**(10) 3194–203
[8] Berti E, Cardoso V and Will C M 2006 *Phys. Rev. D* **73** 064030
[9] Carullo G, Del Pozzo W and Veitch J 2019 *Phys. Rev. D* **99** 123029
[10] Isi M, Giesler M, Farr W M, Scheel M A and Teukolsky S A 2019 *Phys. Rev. Lett.* **123** 111102
[11] Abbott R *et al.* (LIGO Scientific, Virgo) 2021 *Phys. Rev. D* **103** 122002
[12] Abbott R *et al.* (LIGO Scientific, VIRGO, KAGRA) 2021 (*Preprint* `2112.06861`)
[13] Ghosh A, Brito R and Buonanno A 2021 *Phys. Rev. D* **103** 124041
[14] Yu H, Lin Z C and Liu Y X 2019 *Commun. Theor. Phys.* **71** 991–1006
[15] Mishra A K, Ghosh A and Chakraborty S 2021 (*Preprint* `2106.05558`)
[16] Andriot D, Cacciapaglia G, Deandrea A, Deutschmann N and Tsimpis D 2016 *JHEP* **06** 169
[17] Zyla P A *et al.* (Particle Data Group) 2020 *PTEP* **2020** 083C01
[18] Orlando D and Park S C 2010 *JHEP* **08** 006
[19] Starkman G D, Stojkovic D and Trodden M 2001 *Phys. Rev. Lett.* **87** 231303
[20] Chen C M, Ho P M, Neupane I P, Ohta N and Wang J E 2003 *JHEP* **10** 058
[21] Schutz B F and Will C M 1985 *Astrophys. J.* **291** L33
[22] Konoplya R A 2003 *Phys. Rev. D* **68** 024018
[23] Ohashi A and Sakagami M a 2004 *Class. Quant. Grav.* **21** 3973–84
[24] Percival J and Dolan S R 2020 *Phys. Rev. D* **102** 104055
[25] Ferrari V and Mashhoon B 1984 *Phys. Rev. D* **30** 295–304
[26] Dolan S R and Ottewill A C 2009 *Class. Quant. Grav.* **26** 225003
[27] Konoplya R A, Zhidenko A and Zinhailo A F 2019 *Class. Quant. Grav.* **36** 155002
[28] Chen C H, Cho H T, Chrysostomou A and Cornell A S 2021 *Phys. Rev. D* **104**(2) 024009
[29] Zhidenko A 2004 *Class. Quant. Grav.* **21** 273–80
[30] Konoplya R A and Zhidenko A V 2005 *Phys. Lett. B* **609** 377–84